11-1-1994

Three-body analytical potential for interacting helium atoms

Carol A. Parish
University of Richmond, cparish@richmond.edu

Clifford E. Dykstra

Three-body analytical potential for interacting helium atoms

Carol A. Parish and Clifford E. Dykstra

Department of Chemistry, Indiana University Purdue University Indianapolis, Indianapolis, Indiana 46202

Large basis set *ab initio* calculations have been carried out for a dense grid of points on the He_3 potential energy surface. Three-body contributions were extracted at every point, and a number of concise functional representations for the three-body potential surface were then examined. Three-body multipolar dispersion terms and other radial and angular terms were used in the representations, and an assessment of relative importance of the different terms is presented. Combined with a two-body He–He potential, the results of this work should offer a high quality interaction potential for simulations of aggregated helium.

INTRODUCTION

Accurate interaction potentials are a foundation element in the modeling and simulation of weakly bound clusters and ultimately of liquids. Interaction potentials are usually formulated in terms of various N-body interactions. Computational ease may be assured when N is 2, i.e., when only pairwise additive elements are included; but then, accuracy may be compromised. Pairwise additive interaction should be the major contributor to long-range and weak interaction potentials, but nonadditive components may still be important, especially as the size and complexity of the system increases. As well, macroscopic properties, by their very many-body nature, may be sensitive to nonadditivity in the intermolecular interactions. So, the accurate prediction of features from surface phenomena[1-3] to the structure of solids and liquids[4-7] may call for the inclusion of reliable, nonpairwise potential terms.

Three-body and higher order N-body contributions to long-range and weak interaction potentials can arise from some of the same sources as the two-body terms, and this includes polarization, dispersion, and exchange repulsion. Polarization is quite important in a small cluster if there is at least one polar molecule, and it has become routine to evaluate pairwise and nonpairwise polarization energies of clusters of small molecules.[8] In contrast, a cluster of rare-gas atoms exhibits no electrostatic polarization, and so these systems offer a way of isolating nonpolarization contributions to many-body effects.

We recently reported[9] pairwise and many-body contributions to the long-range interaction energies in He_n clusters ($n=1$ to 6) on the basis of high level *ab initio* calculations. Nonpairwise interaction energies at long range were found to grow as the cluster size increases, going from less than 1% in the trimer to nearly 10% in the hexamer. Dipole–dipole–dipole and dipole–dipole–quadrupole dispersion terms were found to comprise a major share of the three-body potential at long range. The current study is a continuation of that work to the close-in regions where the potential becomes strongly repulsive. We focus exclusively on He_3 in order to understand and accurately represent three-body interactions. With this new information, one may achieve a global picture of the role of three-body effects in helium clusters, and this may contribute to the understanding of many-body potentials in general. In addition, the assessment of multipolar dispersion terms vs others may be a guide to the inclusion of three-body effects into model potentials of other rare gases and possibly other systems. Finally, by adding the pair contributions, our representation of the three-body terms offers a good model potential for He_n simulation studies.

THEORETICAL APPROACH

The first aspect of this work was the generation of He_3 potential energy surface points at close-in regions. This extends the previous surface,[9] and the calculational approach is the same. *Ab initio* calculations were carried out using a large basis set, selected previously[9] on the basis of prior *ab initio* studies of He_2[10-23] and their comparison with an experimentally derived dimer potential.[24] This was a $(10s4p2d)$ set of primitive Gaussian functions contracted to $(8s4p2d)$. Wave functions were those of the highly correlated, coupled cluster level with double substitutions (CCD)[25-32] and using a Brueckner orbital reference configuration. The Brueckner orbital CCD method, or B-CCD, was the pair coefficient operator method of Chiles and Dykstra.[33-35]

The B-CCD treatment is size-extensive and is equivalent to the full-CI result in the limit of noninteracting helium atoms. Since the full correlation energy is recovered at the separated limit, the nature of any lingering correlation error will tend to be an undervaluing of the well depth. On the other hand, basis set superposition error (BSSE) will tend to artificially deepen the well. There may be a small advantageous cancellation of lingering error sources in certain regions.

B-CCD energies for the helium dimer were calculated for 182 internuclear separations, which includes the 72 dimer points previously obtained.[9] Dimer interaction energies at each of these points were obtained as the dimer electronic energy less twice the energy of an isolated helium atom. This set of values constitutes the "pair potential" [i.e., $V_2(r)$] of this study. We elected to have at hand a large number of V_2 points rather than a functional fit of a small set of points in order to keep numerical error to a minimum in the analysis of the relatively small three-body effects.

Ab initio calculations on the helium trimer were carried out at the same level of calculation as for the dimer, and

trimer interaction energies were obtained as the difference between the trimer electronic energy and three times the energy of an isolated helium atom. Then, the three-body interaction energy, which we designate V_3, was calculated for each trimer structure as the difference between the trimer interaction energy V and the sum of the pairwise (dimer) potentials. Taking $\mathbf{r}_i$ to be the position vector of atom i, V_3 is simply expressed in the following way:

$$V_3(\mathbf{r}_1,\mathbf{r}_2,\mathbf{r}_3)=V(\mathbf{r}_1,\mathbf{r}_2,\mathbf{r}_3)-V_2(|\mathbf{r}_1-\mathbf{r}_2|)-V_2(|\mathbf{r}_1-\mathbf{r}_3|)$$
$$-V_2(|\mathbf{r}_2-\mathbf{r}_3|). \tag{1}$$

Calculations were carried out for 106 trimer structures, and at all surface points, the separation distance between every pair of helium atoms in the cluster was one of the 182 dimer separations for which V_2 had been obtained. Table I presents a subset of these 182 points that spans the range of separations considered; the complete list is available from the authors on request. Table II[23] gives the V_3 energies.

Instead of expressing the timer potential in terms of position coordinates, it is of course simpler to express it in terms of the atomic separations r_{12}, r_{23}, and r_{13}. These are the lengths of the sides of a triangle, and so the potential must be symmetric with respect to permutation among any of the triangle sides. The 106 trimer surface points, the unique structures studied, correspond to 407 points on the total surface. Of these, 177 were obtained previously.[9] The new points are those for which all three distances were shorter than the calculated dimer equilibrium separation distance of 3.02 Å.[9]

THE HELIUM DIMER POTENTIAL

The highly repulsive, or close-in, region of the helium dimer potential has been studied by Ceperley and Partridge utilizing the Green's function quantum Monte Carlo (QMC) method,[36] and so, comparison of our B-CCD values with their results provides a close-in assessment of basis set and correlation error in the B-CCD values. Table III lists the QMC energies along with the B-CCD energies calculated at the same internuclear separations. The B-CCD energies in this region differ from the QMC energies by up to 3%; however, the shape and form of the B-CCD potential is probably better than the accuracy in the absolute electronic energy. Figure 1 is a plot that compares the QMC energies, the B-CCD energies, the potential of Aziz et al.[37] which was extracted from experimental data, and the ab initio potential of Liu and McLean.[20] The correspondence in the potential shapes is seen to be very good. Though we did not need to find a functional fit of the He_2 curve (i.e., of V_2) in order to isolate three-body effects in the trimer, it is of interest to use the 182 He_2 points for constructing a functional representation. We shall consider that and then return to the trimer surface.

We carried out least-squares fitting of the He_2 energy points to a number of different functional forms. The simplest form was $A\exp(-\beta R)$, and the rms error is given in Table IV. Exponentials with a quadratic dependence on R [e.g., $\exp(-\beta R+\alpha R^2)$] have been used for rare-gas potentials.[38,39] However, in this case, there was only a small

TABLE I. Helium dimer potential energy.

R (Å)	$E_{\text{B-CCD}}$ (a.u.)	$E-E_\infty$ (cm^{-1})
0.661 471 561	−5.242 7877	12 2 002.3
0.793 765 874	−5.464 9519	7 3 241.7
0.926 060 186	−5.600 7500	4 3 436.8
1.058 354 498	−5.682 5963	2 5 473.1
1.094 464 459	−5.698 5129	2 1 979.8
1.162 868 487	−5.723 0837	1 6 586.9
1.231 272 516	−5.741 7806	1 2 483.4
1.299 676 545	−5.755 9681	9369.5
1.368 080 573	−5.766 7050	7013.0
1.436 484 602	−5.774 8094	5234.2
1.450 000 000	−5.776 1566	4938.5
1.500 000 000	−5.780 5304	3978.5
1.550 000 000	−5.784 0784	3199.8
1.600 000 000	−5.786 9524	2569.0
1.650 000 000	−5.789 2773	2058.8
1.700 000 000	−5.791 1557	1646.5
1.750 000 000	−5.792 6712	1313.9
1.800 000 000	−5.793 8924	1045.8
1.850 000 000	−5.794 8754	830.11
1.900 000 000	−5.795 6652	656.74
1.950 000 000	−5.796 2991	517.62
2.000 000 000	−5.796 8068	406.21
2.050 000 000	−5.797 2123	317.18
2.069 788 859	−5.797 3492	287.15
2.100 000 000	−5.797 5356	246.24
2.121 320 344	−5.797 6525	220.59
2.150 000 000	−5.797 7925	189.85
2.191 541 144	−5.797 9649	152.03
2.210 000 000	−5.798 0312	137.45
2.250 000 000	−5.798 1567	109.93
2.262 741 700	−5.798 1918	102.22
2.300 000 000	−5.798 2830	82.203
2.313 293 430	−5.798 3117	75.896
2.333 452 378	−5.798 3519	67.086
2.400 000 000	−5.798 4591	43.549
2.435 045 716	−5.798 5026	33.998
2.474 873 734	−5.798 5433	25.053
2.500 000 000	−5.798 5650	20.305
2.530 949 061	−5.798 5880	15.274
2.570 000 000	−5.798 6118	10.035
2.600 000 000	−5.798 6269	6.726
2.630 000 000	−5.798 6395	3.948
2.660 000 000	−5.798 6501	1.628
2.690 000 000	−5.798 6589	−0.298
2.720 000 000	−5.798 6661	−1.884
2.750 000 000	−5.798 6720	−3.178
2.800 000 000	−5.798 6794	−4.798
2.850 000 000	−5.798 6843	−5.885
2.900 000 000	−5.798 6874	−6.568
3.000 000 000	−5.798 6899	−7.101
3.020 000 000	−5.798 6899	−7.114
3.080 000 000	−5.798 6896	−7.031
3.100 000 000	−5.798 6893	−6.971
3.200 000 000	−5.798 6872	−6.521
3.300 000 000	−5.798 6846	−5.944
3.400 000 000	−5.798 6819	−5.344
3.600 000 000	−5.798 6769	−4.244
3.804 230 000	−5.798 6727	−3.328
4.000 000 000	−5.798 6695	−2.629
4.500 000 000	−5.798 6639	−1.407
5.000 000 000	−5.798 6607	−0.707
5.500 000 000	−5.798 6591	−0.338
6.000 000 000	−5.798 6583	−0.170
7.000 000 000	−5.798 6578	−0.059
9.000 000 000	−5.798 6577	−0.029
12.000 000 000	−5.798 6575	−0.002
18.000 000 000	−5.798 6575	−0.001

TABLE II. Helium trimer three-body potential energy.

R_{12} (Å)	R_{23} (Å)	R_{13} (Å)	V_3 points
1.490	1.49	2.107 178 208	−406.457
1.490	1.49	2.753 161 007	67.537
1.500	1.50	1.826 284 287	−806.314
1.600	1.60	1.948 036 573	−439.619
1.670	1.67	1.670 000 000	−601.251
1.670	1.67	2.200 130 000	−191.898
1.670	1.67	2.777 108 505	−19.356
1.670	1.67	3.085 757 639	17.979
1.700	1.70	2.069 788 859	−236.989
1.700	1.70	3.141 190 411	13.944
1.700	1.70	3.348 346 360	23.68
1.790	1.79	1.790 000 000	−303.302
1.800	1.80	2.191 541 144	−126.713
1.850	1.85	1.850 000 000	−214.643
1.850	1.85	2.616 295 090	−37.386
1.850	1.85	3.418 354 270	2.612
1.850	1.85	3.700 000 000	4.099
1.900	1.90	2.313 293 430	−67.370
1.900	1.90	3.510 742 224	0.934
1.900	1.90	3.742 269 461	1.607
2.000	2.00	1.368 080 573	−279.385
2.000	2.00	2.000 000 000	−89.538
2.000	2.00	2.828 427 125	−13.657
2.000	2.00	3.325 878 449	−3.131
2.000	2.00	3.695 518 130	−0.740
2.000	3.00	3.808 080 000	0.015
2.000	3.50	4.867 170 000	−0.073
2.090	2.09	2.090 000 000	−52.413
2.100	2.10	1.436 484 602	−165.188
2.100	2.10	2.556 798 002	−18.467
2.100	2.10	3.880 294 037	−1.164
2.100	2.10	4.136 192 563	−2.173
2.210	2.21	2.210 000 000	−25.119
2.210	2.21	3.125 410 000	−3.095
2.210	2.21	3.675 095 686	−1.168
2.210	2.21	4.083 547 534	−1.076
2.210	2.21	4.420 000 000	−2.884
2.300	2.30	1.573 292 659	−56.130
2.300	2.30	2.300 000 000	−14.151
2.300	2.30	4.530 115 664	−1.922
2.400	2.40	4.727 077 214	−1.610
2.435	2.00	2.000 000 000	−35.547
2.500	2.50	1.710 100 717	−18.412
2.500	2.50	4.924 038 765	−1.335
2.570	2.57	2.570 000 000	−2.004
2.570	2.57	3.634 530 000	0.061
2.570	2.57	5.140 000 000	−1.512
2.600	2.60	3.676 950 000	0.118
2.600	2.60	5.200 000 000	−1.431
2.630	2.63	3.719 380 000	0.164
2.630	2.63	5.260 000 000	−1.354
2.660	2.66	2.660 000 000	−0.828
2.660	2.66	3.761 808 076	0.200
2.660	2.66	5.320 000 000	−1.280
2.690	2.69	2.690 000 000	−0.595
2.690	2.69	3.804 230 000	0.224
2.690	2.69	5.380 000 000	−1.209
2.700	2.70	4.676 537 180	−0.074
2.720	2.72	2.720 000 000	−0.389
2.720	2.72	3.846 660 000	0.244
2.725	2.72	5.440 000 000	−1.142
2.750	2.75	3.889 090 000	0.263
2.750	2.75	5.500 000 000	−1.077
2.750	3.50	6.250 000 000	−0.514
2.750	4.50	7.250 000 000	−0.157
2.900	2.90	5.022 947 342	−0.057
3.000	2.75	3.200 210 000	0.254

TABLE II. (Continued.)

R_{12} (Å)	R_{23} (Å)	R_{13} (Å)	V_3 points
3.000	2.80	2.900 190 000	0.187
3.000	2.80	3.000 000 000	0.224
3.000	3.00	4.000 000 000	0.268
3.000	3.00	4.596 270 000	0.170
3.000	3.00	5.638 160 000	−0.277
3.000	3.00	6.000 000 000	−0.628
3.000	3.27	3.495 040 000	0.158
3.000	3.50	6.500 000 000	−0.388
3.000	3.60	3.996 550 000	0.195
3.000	3.60	5.500 000 000	−0.046
3.000	4.00	5.000 000 000	0.090
3.000	4.00	6.000 000 000	−0.076
3.000	4.00	7.000 000 000	−0.263
3.000	4.50	4.500 260 000	0.143
3.000	5.00	5.000 260 000	0.069
3.000	5.00	8.000 000 000	−0.066
3.000	5.70	5.100 240 000	0.019
3.000	5.70	6.000 000 000	0.008
3.000	6.00	9.000 000 000	−0.010
3.000	9.00	12.000 000 000	0.016
3.000	12.00	15.000 000 000	0.000
3.250	3.75	7.000 000 000	−0.266
3.250	4.50	7.750 000 000	−0.126
3.300	3.30	2.257 332 946	0.138
3.500	3.50	2.394 141 003	0.259
3.500	3.50	7.000 000 000	−0.267
3.500	4.00	7.500 000 000	−0.193
3.500	4.25	7.750 000 000	−0.156
3.500	4.75	8.250 000 000	−0.083
3.700	3.70	2.530 949 061	0.286
4.000	4.00	8.000 000 000	−0.154
4.000	4.50	8.500 000 000	−0.093
4.000	5.00	9.000 000 000	−0.036
4.500	4.50	9.000 000 000	−0.052
4.500	5.00	9.500 000 000	−0.016
4.750	6.00	10.750 000 000	−0.003
5.000	5.00	10.000 000 000	−0.004
6.000	6.00	12.000 000 000	−0.000
6.000	12.00	18.000 000 000	0.000

improvement in the quality of the fit as indicated by the rms error in Table IV. A sum of three inverse even powers (e.g., r^{-6}, r^{-8}, r^{-10}) offered a better representation than a single exponential. Scaling that sum by an exponential offered further improvement, but the best concise functional fit from a distance of 1.3 Å outward was that used by Ceperley and

TABLE III. Quantum Monte Carlo energies (Ref. 36) and B-CCD energies of He_2 at close-in separations.

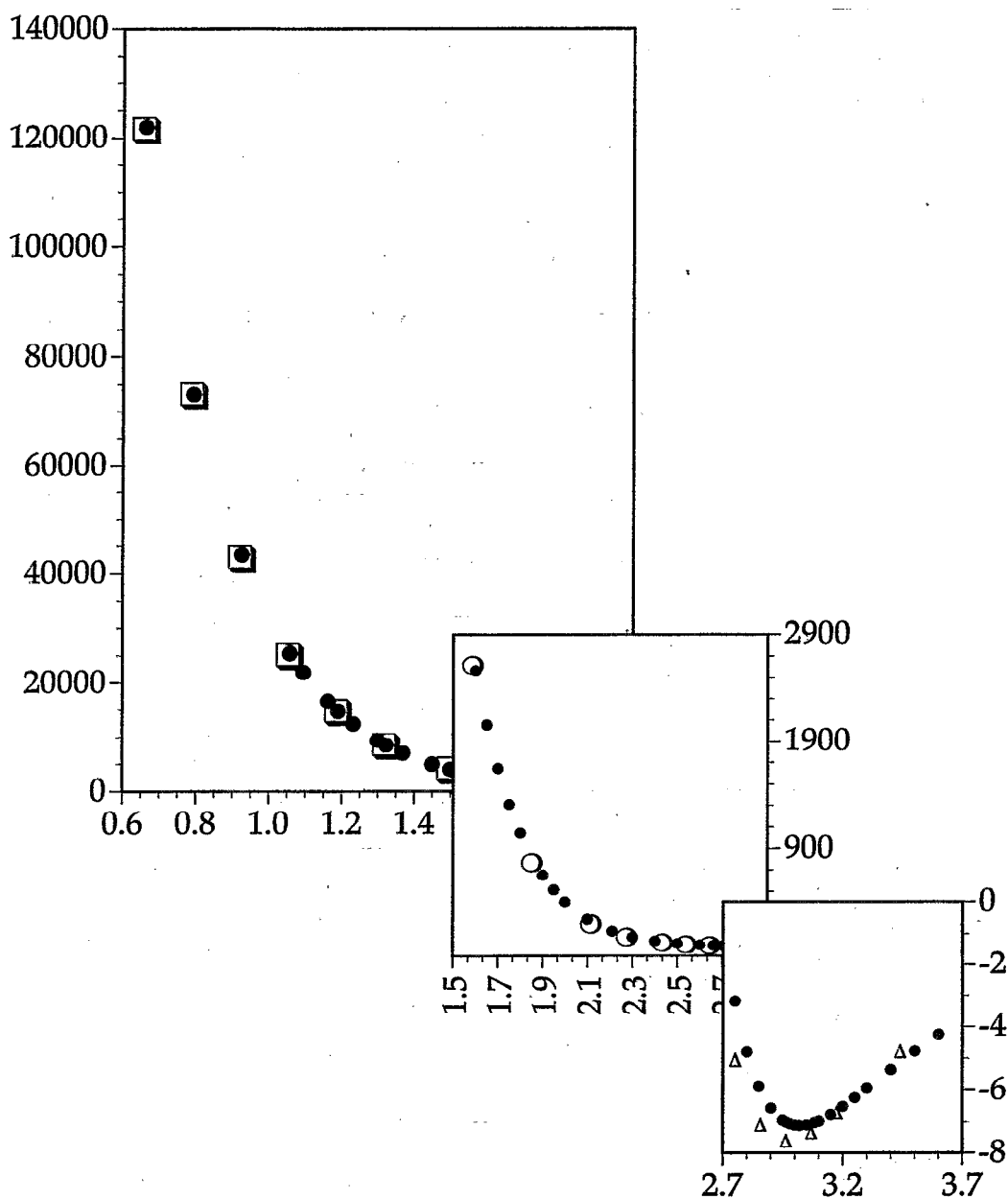| r (Å)	E(QMC) (cm^{-1})	E(BCCD) (cm^{-1})	Difference (cm^{-1})	Difference %
0.661 471 561	121 370.245	122 002.311	632	0.52
0.793 765 874	72 974.905	73 241.707	266	0.36
0.926 060 186	42 686.665	43 436.754	750	1.75
1.058 354 498	24 908.785	25 473.108	564	2.26
1.190 648 810	14 571.277	14 783.554	212	1.45
1.322 943 123	8 294.149	8 492.942	198	2.39
1.500 005 830	3 860.653	3 978.441	117	3.03
1.587 531 747	2 653.513	2 714.087	60	2.26

FIG. 1. He$_2$ potential in cm^{-1}. The solid circles are the B-CCD calculations. The open squares in the close-in region are the QMC calculations of Ceperley and Partridge (Ref. 36). The open circles are based on experiment (Ref. 37), and the open triangles are the exhaustive or limiting *ab initio* calculational results of Liu and McLean (Ref. 20). In both the middle and rightmost parts of the figure, plotting both the values of Aziz *et al.* (Ref. 37) and Liu and McLean would show these curves to be coincident on the scale of the figure.

Partridge[36] to fit QMC energies in the highly repulsive region:

$$V(r) = \exp^{-\beta r} \sum_{k=-1}^{4} a_k r^k. \tag{2}$$

With this functional form, the rms error was 0.3 cm^{-1}. Of course, this functional form does not have the explicit 1/r^6 term of dipole–dipole dispersion that should be the longest-range interaction between two helium atoms. It represents more of a practical than physical choice for the form of the

potential. The fact that it serves to represent the dimer potential quite well highlights the difficulty of using surface fitting to extract true multipolar dispersion coefficients. We can see this from the "6–8–10" fit of the dimer potential (Table IV) where the c_6, c_8, and c_{10} coefficients that are optimum over the stated range of distances are considerably different than the explicitly calculated multipolar dispersion coefficients of Thakkar.[40]

The well depth and equilibrium separation of our *ab initio* potential are -7.428 cm^{-1} and 3.033 Å, respectively. In

TABLE IV. Functional fits of the calculated He_2 potential energies.

Function	rms error (cm^{-1})		Parameter values
	$0.6 < r(Å) < 1.6$	$1.3 < r(Å) < 16$	$1.3 < r(Å) < 16$
$V(r) = A\ e^{-\beta r}$	401	19.3	$\beta = 4.35$
			$A = 268\ 8503$
$V(r) = c_0 + \dfrac{c_6}{r^6} + \dfrac{c_8}{r^8} + \dfrac{c_{10}}{r^{10}}$	218	18.0	$c_0 = -5.901\ 5747$
			$c_6 = -27\ 258.228$
			$c_8 = 289\ 384.53$
			$c_{10} = -283\ 091.43$
$V(r) = e^{-4.35r}\left(c_0 + \dfrac{c_6}{r^6} + \dfrac{c_8}{r^8} + \dfrac{c_{10}}{r^{10}} \right)$	41.3	11.2	$c_0 = 2\ 199\ 509$
			$c_6 = 44\ 666\ 817$
			$c_8 = -133\ 793\ 955$
			$c_{10} = 105\ 138\ 760$
$V(r) = A\ e^{-(\beta r + \alpha r^2)}$	221	8.97	$\beta = 3.50$
			$\alpha = 0.285$
			$A = 1\ 435\ 858$
$V(r) = e^{-\beta r} \displaystyle\sum_{k=-1}^{4} a_k r^k$	0.013	0.29	$a_{-1} = 84\ 139.61$
			$a_0 = 1\ 410\ 276$
			$a_1 = -1\ 290\ 504$
			$a_2 = 406\ 603.1$
			$a_3 = -47\ 421.51$
			$a_4 = 196.6650$
			$\beta = 2.85$

comparison, the corresponding potential parameters deduced from experimental results[37] are -7.611 cm^{-1} and 2.963 Å. The very extensive, limiting *ab initio* calculations of Liu and McLean[20] yielded -7.605 cm^{-1} for the well depth and 2.969 Å for the equilibrium separation. Our equilibrium distance, though 0.07 Å too long, corresponds to an energetic error of only about 0.4 cm^{-1} as this is the energy we obtain at a distance of 2.963 Å relative to our equilibrium value.

THE HELIUM THREE-BODY POTENTIAL

We have already reported on many-body effects in clusters of helium atoms at long range.[9] We found that the many-body or nonpairwise contributions tend to be less than a few percent of the overall attractive interaction in regions near the minima. These contributions can be represented with a small number of terms that include an Axilrod–Teller[41] dipole–dipole–dipole (DDD) dispersion term, along with the next higher multipole dispersion term,[42] dipole–dipole–quadrupole (DDQ), plus several terms from a power series expansion in the radial and angular coordinates. And it was found important to include as an independent term one part of the DDD term, namely $1/r_{12}^3 r_{23}^3 r_{13}^3$.

The analysis of three-body dispersion by Axilrod and Teller[41] predicts a repulsive contribution for an equilateral triangular arrangement of three like atoms and an attractive contribution for a symmetric, linear arrangement. This qualitative conclusion was supported by our earlier results on the attractive region of the potential. However, three-body non-additivity in the close-in, repulsive regions seems dominated by the exchange repulsion which has been shown[43] to behave in an opposite fashion.

The previously determined[9] attractive representation, and then other functional forms, were applied to the extended potential surface generated here. The previously used potential[9] was not flexible enough to adequately describe both the attractive and repulsive regions; fitting yielded an rms deviation of 3.98 cm^{-1}. Let us consider the fitting of V_3 by terms in order of their importance in diminishing the rms error of the fit.

The best one-term functional fit was to a simple function, f_1, that describes the radial dependence of the Axilrod and Teller function:

$$f_1 = \frac{1}{r_{12}^3 r_{23}^3 r_{13}^3}. \tag{3}$$

The rms error was 21.3 cm^{-1}. The most significant improvement in the fit was achieved by including the angular dependence of the Axilrod and Teller function via a function we designate as f_2:

$$f_2 = \frac{\cos\theta_{12}\cos\theta_{23}\cos\theta_{13}}{r_{12}^3 r_{23}^3 r_{13}^3}. \tag{4}$$

The angle subscript identifies the angle which is opposite a particular side of the triangle composed of the three atoms. The rms deviation with the two-term function $c_1 f_1 + c_2 f_2$ was 10.5 cm^{-1}. The next improvement in the description of the three-body energies was achieved by including the dipole–dipole–quadrupole (DDQ) term, which is the next higher multipole dispersion term:

$$f_3 = (1 + P_{12\ 13} + P_{12\ 23})\ \frac{9\cos\theta_{12} - 25\cos(3\theta_{12}) + 6\cos(\theta_{23} - \theta_{13})[3 + 5\cos(2\theta_{12})]}{r_{12}^3 r_{23}^4 r_{13}^4}. \tag{5}$$

The P operators interchange variable subscripts so that the symmetry of the potential is preserved. The rms error for the three term fit was 4.20 cm^{-1}. The fourth and fifth most important terms in the attractive region were

$$g_4 = \frac{\cos\theta_{12}\cos\theta_{23}\cos\theta_{13}}{r_{12}^4 r_{23}^4 r_{13}^4}, \tag{6}$$

$$g_5 = \frac{\cos\theta_{12}\cos\theta_{23}\cos\theta_{13}}{r_{12}^5 r_{23}^5 r_{13}^5}. \tag{7}$$

But, these were not the next most important in improving the fit of the entire surface. Instead, the next most important function was a radial function, f_4:

$$f_4 = (1 + P_{12\ 13} + P_{12\ 23}) \frac{1}{r_{12}^2 r_{23}^2 r_{13}^5}. \tag{8}$$

The rms deviation for the four term fit was 3.47 cm^{-1}.

If instead of f_4, the fourth term in the fit is the dipole–quadrupole–quadrupole (DQQ) dispersion,[42] the quality of the fit corresponds to an rms error of 3.79 cm^{-1}. Most of the improvement develops at long range, not close-in, whereas the function f_4 is a somewhat better term in the representa-

tion overall. If the DQQ and QQQ terms are included with the DDQ term (no f_4), a fit with an rms error of 2.82 cm^{-1} is achieved. These terms together seem balanced at representing the potential close-in and at long range, but we found a different functional form would work still better.

An additional radial term and then the terms g_4 and g_5 that were important at long range were included. The rms error was reduced to 0.52 cm^{-1}. So, the final function for V_3 is

$$V_3 = C_1 \frac{1}{r_{12}^3 r_{23}^3 r_{13}^3} + C_2 \frac{\cos \theta_{12} \cos \theta_{23} \cos \theta_{13}}{r_{12}^3 r_{23}^3 r_{13}^3} + C_3 (1 + P_{12\ 13} + P_{12\ 23})$$

$$\times \frac{9 \cos \theta_{12} - 25 \cos(3\theta_{12}) + 6 \cos(\theta_{23} - \theta_{13})[3 + 5 \cos(2\theta_{12})]}{r_{12}^3 r_{23}^4 r_{13}^4} + C_4 (1 + P_{12\ 13} + P_{12\ 23}) \frac{1}{r_{12}^2 r_{23}^2 r_{13}^5}$$

$$+ C_5 (1 + P_{12\ 13} + P_{12\ 23}) \frac{1}{r_{12}^1 r_{23}^1 r_{13}^5} + C_6 \frac{\cos \theta_{12} \cos \theta_{23} \cos \theta_{13}}{r_{12}^4 r_{23}^4 r_{13}^4} + C_7 \frac{\cos \theta_{12} \cos \theta_{23} \cos \theta_{13}}{r_{12}^5 r_{23}^5 r_{13}^5}$$

$$+ C_8 (1 + P_{12\ 13} + P_{12\ 23}) \frac{1}{r_{12}^2 r_{23}^2 r_{13}^3} + C_9 (1 + P_{12\ 13} + P_{12\ 23} + P_{23\ 13} + P_{12\ 23} P_{23\ 13} + P_{12\ 23} P_{12\ 13}) \frac{1}{r_{12}^1 r_{23}^3 r_{13}^5},$$

where in units of cm^{-1} and Å the coefficients are $C_1 = -194\ 219.60$, $C_2 = 322\ 529.34$, $C_3 = 683.883\ 83$, $C_4 = -256\ 800.13$, $C_5 = -1445.9536$, $C_6 = -2\ 433\ 561.9$, $C_7 = 6\ 698\ 227.6$, $C_8 = 24\ 919.062$, $C_9 = 125\ 677.98$. The deviation for close-in points was only 0.68 cm^{-1} and for long-range points was only 0.15 cm^{-1}. If the additional flexibility of DQQ and QQQ terms is incorporated, the rms error is reduced only slightly more, to 0.34 cm^{-1}. Whereas the DDQ term seems essential throughout, the DQQ and QQQ terms' importance at long range seems to be somewhat outweighed close-in by other terms. Of course, the practical consequence of this work is the analytic representation of the three-body potential in helium clusters rather than the true long-range multipolar dispersion coefficients. Again, potential surface fitting is not an ideal means for finding the dispersion coefficients, and so, it is not surprising that the C_2 and C_3 values given above are quite different than the directly calculated DDD and DDQ coefficients of Thakkar.[40]

The B-CCD calculated equilibrium structure of He$_3$ is that of an equilateral triangle with an atom–atom separation distance of 3.02 Å and a well depth of 21.1 cm^{-1}. At the equilibrium, the three-body effects are destabilizing, though only by 0.27 cm^{-1}. The total electron correlation contribution to the stabilization energy at the equilibrium is 35.7 cm^{-1} at the B-CCD level. This is greater than the well depth, of course, because the SCF interaction energy is repulsive at the 3.02 Å equilateral triangle structure relative to three separated atoms.

The nature of the correlation effects is interesting in other ways. In the course of obtaining B-CCD energies, we also obtained CCD energies (double substitution coupled cluster values with SCF reference orbitals rather than

Brueckner orbitals). The difference between the two levels is an effect of single, triple, and quintuple substitutions. Throughout much of the surface, the differences between B-CCD and CCD energies are around 0.5 cm^{-1}; for instance, at the equilibrium the difference is 0.67 cm^{-1}. The extremes in the difference are that it is at its smallest size close-in, diminishing to about 0.26 cm^{-1}, and at its largest size, up to about 1 cm^{-1}, when two atoms are close and the third is well removed from both. The CCD vs B-CCD differences are very small fractions of the total electronic energies, and they are no more than a few percent of the correlation contribution to the stability of the He$_3$ equilibrium structure. In view of that, it is unlikely that significant refinement in three-body potentials would come about from going beyond B-CCD. This is supported by information from the opposite direction: At the level of second order many-body perturbation theory, MBPT2, we find that the correlation contribution to the stability of equilibrium He$_3$ is 32.2 cm^{-1} or 90% of the B-CCD correlation contribution (92% of CCD). Furthermore, the three-body effect on the He$_3$ equilibrium structure's energy is a destabilization of 0.29 cm^{-1}, for which the corresponding B-CCD value is a very similar 0.27 cm^{-1}. On that basis, we believe that the functional fit of V_3 presented above should be quite accurate for He$_n$ simulations, especially when combined with the best possible pair potential.

[1] K. Ebina and M. Kaburagi, Surf. Sci. **242**, 124 (1991).
[2] R. A. Aziz, U. Buck, H. Jonsson, J.-C. Ruiz-Suarez, B. Schmidt, G. Scoles, M. J. Slaman, and J. Xu, J. Chem. Phys. **91**, 6477 (1989).
[3] M. B. Doran and I. J. Zucker, J. Phys. C **4**, 307 (1971); I. J. Zucker and M. B. Doran, *ibid.* **5**, 2302 (1972).
[4] N. Pastor and I. Ortega-Blake, J. Chem. Phys. **99**, 7899 (1993).

[5] D. J. Chartrand, R. J. LeRoy, A. Kumar, and W. J. Meath, J. Chem. Phys. **98**, 5668 (1993).

[6] P. J. Haskins and M. D. Cook, in *Shock Compression of Condensed Matter*, edited by S. C. Schmidt, R. D. Dick, J. W. Forbes, and D. G. Tasker (Elsevier, Amsterdam, 1992), p. 135.

[7] M. Tau, L. Reatto, R. Magli, P. A. Egelstaff, and F. Barocchi, J. Phys. Condensed Matter **1**, 7131 (1989).

[8] C. E. Dykstra, Chem. Rev. **93**, 2339 (1993).

[9] C. A. Parish and C. E. Dykstra, J. Chem. Phys. **98**, 437 (1993).

[10] H. F. Schaefer, D. R. McLaughlin, F. E. Harris, and B. J. Alder, Phys. Rev. Lett. **25**, 988 (1970).

[11] B. Liu and A. D. McLean, J. Chem. Phys. **59**, 4557 (1973).

[12] J. N. Murrell and A. J. C. Varandas, Mol. Phys. **30**, 223 (1975).

[13] P. G. Burton, J. Chem. Phys. **67**, 4696 (1977); **70**, 3112 (1979).

[14] P. D. Dacre, Mol. Phys. **36**, 541 (1978).

[15] C. E. Dykstra, J. Chem. Phys. **68**, 1829 (1978).

[16] P. Cremaschi, G. Morosi, M. Raimondi, and M. Simonetta, Mol. Phys. **38**, 1555 (1979).

[17] J. R. Collins and G. A. Gallup, Mol. Phys. **49**, 871 (1983).

[18] J. R. Collins and G. A. Gallup, Chem. Phys. Lett. **123**, 56 (1986).

[19] J. H. van Lenthe, R. J. Vos, J. C. G. M. van Duijneveldt-van de Rijdt, and F. B. van Duijneveldt, Chem. Phys. Lett. **143**, 435 (1988).

[20] B. Liu and A. D. McLean, J. Chem. Phys. **91**, 2348 (1989).

[21] S. Rybak, K. Szalewicz, and B. Jeziorski, J. Chem. Phys. **91**, 4779 (1989).

[22] W. Rijks, M. Gerritsen, and P. E. S. Wormer, Mol. Phys. **66**, 929 (1989).

[23] R. J. Vos, J. H. van Lenthe, and F. B. van Duijneveldt, J. Chem. Phys. **93**, 643 (1990).

[24] J. M. Farrar and Y. T. Lee, J. Chem. Phys. **56**, 5801 (1972); A. L. J. Burgmans, J. M. Farrar, and Y. T. Lee, *ibid.* **64**, 1345 (1976).

[25] J. Cizek, J. Chem. Phys. **45**, 4256 (1966); Adv. Chem. Phys. **14**, 35 (1969).

[26] J. Cizek, J. Paldus, and L. Sroubkova, Int. J. Quantum Chem. **3**, 149 (1969).

[27] A. C. Hurley, *Electron Correlation in Small Molecules* (Academic, New York, 1976).

[28] R. J. Bartlett and G. D. Purvis, Int. J. Quantum Chem. **14**, 561 (1978).

[29] I. Lindgren, Int. J. Quantum Chem. Symp. **12**, 33 (1978).

[30] R. J. Bartlett, Annu. Rev. Phys. Chem. **32**, 359 (1981).

[31] B. Heriorski and H. J. Monkhorst, Phys. Rev. A **24**, 1668 (1981).

[32] R. J. Bartlett, J. Paldus, and C. E. Dykstra, in *Advanced Theories and Computational Approaches to the Electronic Structure of Molecules*, edited by C. E. Dykstra (Reidel, Dordrecht, 1984).

[33] R. A. Chiles and C. E. Dykstra, J. Chem. Phys. **74**, 4544 (1981).

[34] C. E. Dykstra, *Ab Initio Calculation of the Structures and Properties of Molecules* (Elsevier, Amsterdam, 1988).

[35] C. E. Dykstra, Chem. Phys. Lett. **88**, 202 (1982).

[36] D. M. Ceperley and H. Partridge, J. Chem. Phys. **84**, 820 (1986).

[37] R. A. Aziz, F. R. W. McCourt, and C. C. K. Wong, Mol. Phys. **61**, 1487 (1987).

[38] C. Douketis, G. Scoles, S. Marchetti, M. Zen, and A. J. Thakkar, J. Chem. Phys. **76**, 3057 (1982).

[39] R. A. Aziz and M. J. Slaman, J. Chem. Phys. **94**, 8047 (1991).

[40] A. J. Thakkar, J. Chem. Phys. **75**, 4496 (1981).

[41] B. M. Axilrod and E. Teller, J. Chem. Phys. **11**, 299 (1943).

[42] W. J. Meath and M. Koulis, J. Mol. Struct. (THEOCHEM) **226**, 1 (1991); W. J. Meath and R. A. Aziz, Mol. Phys. **52**, 225 (1984).

[43] M. Szczesniak and G. Chalasinski, J. Mol. Struct. (THEOCHEM) **261**, 37 (1992).